or rBsep- (B) and GFP-enriched membrane vesicles, respectively.

(C, D) The concentration-dependent uptake of FEX by hBSEP (C) and rBsep (D) was examined at 37 °C in the medium containing 5 mM ATP (closed columns) or AMP (open columns). Each point and vertical bar represents the mean ± S.E. (n=3). Where no vertical bars are shown, the S.E. values were contained within the limits of symbols. *: $p<0.05$, **: $p<0.01$

Figure 3. Plasma concentration, biliary excretion rate and urinary excretion rate of FEX during constant intravenous infusion into FVB mice and Mrp2 (-/-) mice.

The plasma concentration (A), biliary excretion rate (B) and urinary excretion rate (C) of FEX were determined during constant intravenous infusion into FVB mice (open circles) and Mrp2 (-/-) mice (closed circles). Each point and vertical bar represents the mean ± S.E. (FVB mice, n=5; Mrp2 (-/-) mice, n=6). *: $p<0.05$, **: $p<0.01$

Figure 4. The uptake of FEX in the membrane vesicles prepared from hMRP3- (A, C) and hMRP4- (B) expressing HEK293 cells.

(A, B) The uptake of 10 μM FEX by hMRP3 (A) and hMRP4 (B) was examined at 37 °C in the medium containing 5 mM ATP (closed symbols) or AMP (open symbols). Circles and squares represent the uptake in hMRP3- (A) or hMRP4- (B) and GFP-enriched membrane vesicles, respectively.

(C) The concentration-dependent uptake of FEX by hMRP3 was examined at 37 °C in the medium containing 5 mM ATP (closed columns) or AMP (open columns). Each point and vertical bar represents the mean ± S.E. (n=3). Where no vertical bars are shown, the S.E. values were contained within the limits of symbols. **: $p<0.01$

Figure 5 Plasma concentration, biliary excretion rate and urinary excretion rate of FEX during constant intravenous infusion into FVB mice and Mrp3 (-/-) mice.

The plasma concentration (A), biliary excretion rate (B) and urinary excretion rate (C) of FEX were determined during constant intravenous infusion into FVB mice (open circles) and Mrp3 (-/-) mice (closed circles). Each point and vertical bar represents the mean ± S.E. (FVB mice, n=7; Mrp3 (-/-) mice, n=6). Where no vertical bars are shown, the S.E. values were contained within

the limits of symbols. *: $p<0.05$, **: $p<0.01$

Figure 6 Plasma concentration, biliary excretion rate and urinary excretion rate of FEX during constant intravenous infusion into C57BL/6 mice and Mrp4 (-/-) mice.

The plasma concentration (A), biliary excretion rate (B) and urinary excretion rate (C) of FEX were determined during constant intravenous infusion into C57BL/6 mice (open circles) and Mrp4 (-/-) mice (closed circles). Each point and vertical bar represents the mean ± S.E. (C57BL/6 mice, n=4; Mrp4 (-/-) mice, n=3). Where no vertical bars are shown, the S.E. values were contained within the limits of symbols.

Figure 7 Comparison of the protein expression levels of various transporters expressed in the crude membrane of mouse liver between FVB mice and Mrp3 (-/-) mice using Western blot analyses.

The expression levels of the efflux transporters expressed in liver canalicular membrane (A) and sinusoidal membrane (B) in the hepatic crude membrane fraction prepared from five FVB mice and Mrp3 (-/-) mice were

determined by Western blot analyses. β-actin was used for the normalization of the expression level of each transporter.

Figure 8. Schematic diagrams of the proposed transport mechanisms of FEX in wild-type, Mrp2(-/-) and Mrp3(-/-) mice

FEX is a substrate of hOATPs, hMRP2, hMRP3, hBSEP, and P-gp in humans. In this figure, it is assumed that there is no difference in the substrate specificity of each transporter for FEX between humans and mice. In the Mrp2 (-/-) mice, the expression levels of Mrp3 and Mrp4 are increased compared with those in the wild-type mice. In the Mrp3 (-/-) mice, the unidentified transporter(s) may be increased compared with the wild-type mice.

Table 1. Nucleotide sequences of the primers used in real-time quantitative PCR.

Transporter	Forward primer	Reverse primer
Oatp1a1	cagataaatggatttgccag	gtcaacaaatagttacagag
Oatp1a4	atagcttcaggcgcatttac	ttctccatcattctgcatcg
Oatp1b2	ttcaccacaacaatggccta	ttttccccacagacaggttc
Mrp2	tctctggtttgcctgtta	gcagaagacaatcaggttt
Mrp3	gctctcacaaggtggtacaa	caggttgaaacaggcactca
Mrp4	gatcgcctacgtttctcagc	ccggtctcctataaccgtca
Mdr1a	tcattgcgatagctggag	caaacttctgctcccgagtc
Mdr1b	acctgctgttggcgtatttg	ttcctccagactgctgttgc
Bcrp	aaatggagcacctcaacctg	cccatcacaacgtcatcttg
Bsep	aaatcggatggtttgactgc	tgacagcgagaatcaccaag
Mate1	aacaccatctcccagtttgc	gccaaggataccactcagga
G3pdh	tgcgacttcaacagcaactc	cttgctcagtgtccttgctg

Table 2. Pharmacokinetic parameters of FEX during constant intravenous infusion into FVB mice (n=5) and Mrp2 (-/-) mice (n=6).

Parameters	FVB mice (n=5)	Mrp2 (-/-) mice (n=6)
C_{ss} (nM) [1)]	414 ± 54	597 ± 49*
$CL_{tot,plasma}$ (mL/min/kg b.w.)	29.8 ± 3.9	20.1 ± 1.4*
$CL_{bile,plasma}$ (mL/min/kg b.w.)	9.48 ± 0.82	3.38 ± 0.38**
$CL_{bile,liver}$ (mL/min/kg b.w.)	0.250 ± 0.053	0.198 ± 0.022
V_{bile} (nmol/min/kg b.w.)	3.71 ± 0.32	1.93 ± 0.14**
Bile flow rate (μL/min/kg b.w.)	64.0 ± 7.1	53.1 ± 4.6
$K_{p,liver}$	40.7 ± 6.8	16.2 ± 2.0*
$CL_{urine,p}$ (mL/min/kg b.w.)	16.9 ± 2.3	15.2 ± 3.2
V_{urine} (nmol/min/kg b.w.)	6.59 ± 0.91	8.66 ± 1.79
GFR (mL/min/kg b.w.) [2)]	17.3 ± 0.9	17.7 ± 2.5
$K_{p,kidney}$	22.7 ± 4.4	21.8 ± 3.1
$K_{p,brain}$	0.0183 ± 0.0028	0.0190 ± 0.0043

Data represent the mean ± S.E. (n=5 or 6). The meanings of these parameters are explained in the "**Materials & Methods**" section.

1) Corrected steady-state plasma concentration at the infusion rate of 700 nmol/hr/kg

2) GFR represents the glomerular filtration rate.

*: $p<0.05$, **: $p<0.01$

Table 3. Pharmacokinetic parameters of FEX during constant intravenous infusion into FVB mice (n=7) and Mrp3 (-/-) mice (n=6).

Parameters	FVB mice (n=7)	Mrp3 (-/-) mice (n=6)
C_{ss} (nM) [1)]	382 ± 46	214 ± 11**
$CL_{tot,plasma}$ (mL/min/kg b.w.)	33.6 ± 3.8	56.1 ± 3.1**
$CL_{bile,plasma}$ (mL/min/kg b.w.)	9.32 ± 1.01	25.9 ± 1.1**
$CL_{bile,liver}$ (mL/min/kg b.w.)	0.235 ± 0.025	0.495 ± 0.023**
V_{bile} (nmol/min/kg b.w.)	3.17 ± 0.27	5.64 ± 0.19**
Bile flow rate (μL/min/kg b.w.)	53.7 ± 3.4	88.6 ± 7.4*
$K_{p,liver}$	37.9 ± 3.4	48.0 ± 2.1*
$CL_{urine,p}$ (mL/min/kg b.w.)	14.2 ± 2.3	19.0 ± 1.8
V_{urine} (nmol/min/kg b.w.)	4.84 ± 0.91	4.11 ± 0.30
GFR (mL/min/kg b.w.) [2)]	15.1 ± 2.1	19.9 ± 1.8
$K_{p,kidney}$	23.5 ± 2.3	24.8 ± 2.1
$K_{p,brain}$	0.0169 ± 0.0016	0.0171 ± 0.0021

Data represent the mean ± S.E. (n=6 or 7). The meanings of these parameters are explained in the "**Materials & Methods**" section.

1) Corrected steady-state plasma concentration at the infusion rate of 700 nmol/hr/kg

2) GFR represents the glomerular filtration rate.

*: $p<0.05$, **: $p<0.01$

Table 4. Pharmacokinetic parameters of FEX during constant intravenous infusion into C57BL/6 mice (n=4) and Mrp4 (-/-) mice (n=3).

Parameters	C57BL/6 mice (n=4)	Mrp4 (-/-) mice (n=3)
C_{ss} (nM) [1)]	480 ± 49	382 ± 29
$CL_{tot,plasma}$ (mL/min/kg b.w.)	25.5 ± 2.9	31.1 ± 2.2
$CL_{bile,plasma}$ (mL/min/kg b.w.)	10.9 ± 1.5	15.3 ± 1.1
$CL_{bile,liver}$ (mL/min/kg b.w.)	0.369 ± 0.033	0.454 ± 0.025
V_{bile} (nmol/min/kg b.w.)	5.50 ± 0.26	5.50 ± 0.18
Bile flow rate (μL/min/kg b.w.)	71.1 ± 11.1	76.6 ± 2.2
$K_{p,liver}$	28.3 ± 3.7	29.5 ± 0.4
$CL_{urine,p}$ (mL/min/kg b.w.)	14.7 ± 1.3	17.2 ± 3.1
V_{urine} (nmol/min/kg b.w.)	7.69 ± 0.80	6.13 ± 0.85
GFR (mL/min/kg b.w.) [2)]	13.6 ± 1.2	12.8 ± 2.4
$K_{p,kidney}$	15.6 ± 1.5	15.6 ± 1.7
$K_{p,brain}$	0.0210 ± 0.0015	0.0210 ± 0.0021

Data represent the mean ± S.E. (n=3 or 4). The meanings of these parameters are explained in the "**Materials & Methods**" section.

1) Corrected steady-state plasma concentration at the infusion rate of 700 nmol/hr/kg

2) GFR represents the glomerular filtration rate.

Table 5. Comparison of mRNA levels of various transporters expressed in mouse liver, bile flow rate, excretion rate and efflux clearance based on the liver concentration of GSH and total bile acids between FVB mice (n=3) and Mrp3 (-/-) mice (n=3).

Parameters		FVB mice	Mrp3 (-/-) mice
mRNA expression level normalized by the expression level of mGapdh	mOatp1a1	5.20 ± 0.63	5.66 ± 0.34
	mOatp1a4	1.44 ± 0.17	1.42 ± 0.20
	mOatp1b2	4.35 ± 0.12	3.02 ± 0.43*
	mMrp3	1.03 ± 0.21	n.d. [1)]
	mMrp4	0.0460 ± 0.0243	0.0255 ± 0.0032
	mMrp2	18.8 ± 2.2	17.8 ± 1.73
	mMdr1a	0.431 ± 0.064	0.231 ± 0.006
	mMdr1b	0.319 ± 0.061	0.356 ± 0.117
	mBcrp	0.610 ± 0.064	0.796 ± 0.018*
	mBsep	11.3 ± 1.5	10.7 ± 1.1
	mMate1	0.779 ± 0.038	0.620 ± 0.042*
bile flow rate (μL/min/kg)		51.9 ± 8.6	81.1 ± 3.5*
hepatic GSH concentration (mM)		4.27 ± 0.75	5.62 ± 0.13
GSH excretion rate (nmol/min/kg)		231 ± 37	300 ± 54
GSH efflux clearance (μL/min/kg)		54.8 ± 3.3	53.3 ± 9.1
total bile acids excretion rate (μmol/min/kg)		4.21 ± 0.64	3.81 ± 0.28
total bile acids efflux clearance (μL/min/kg)		498 ± 67	486 ± 28

Data represent the mean ± S.E. (n=3). The meanings of these parameters are explained in the "**Materials & Methods**" section.

1) n.d. represents not detected.

*: $p<0.05$

Figure 1

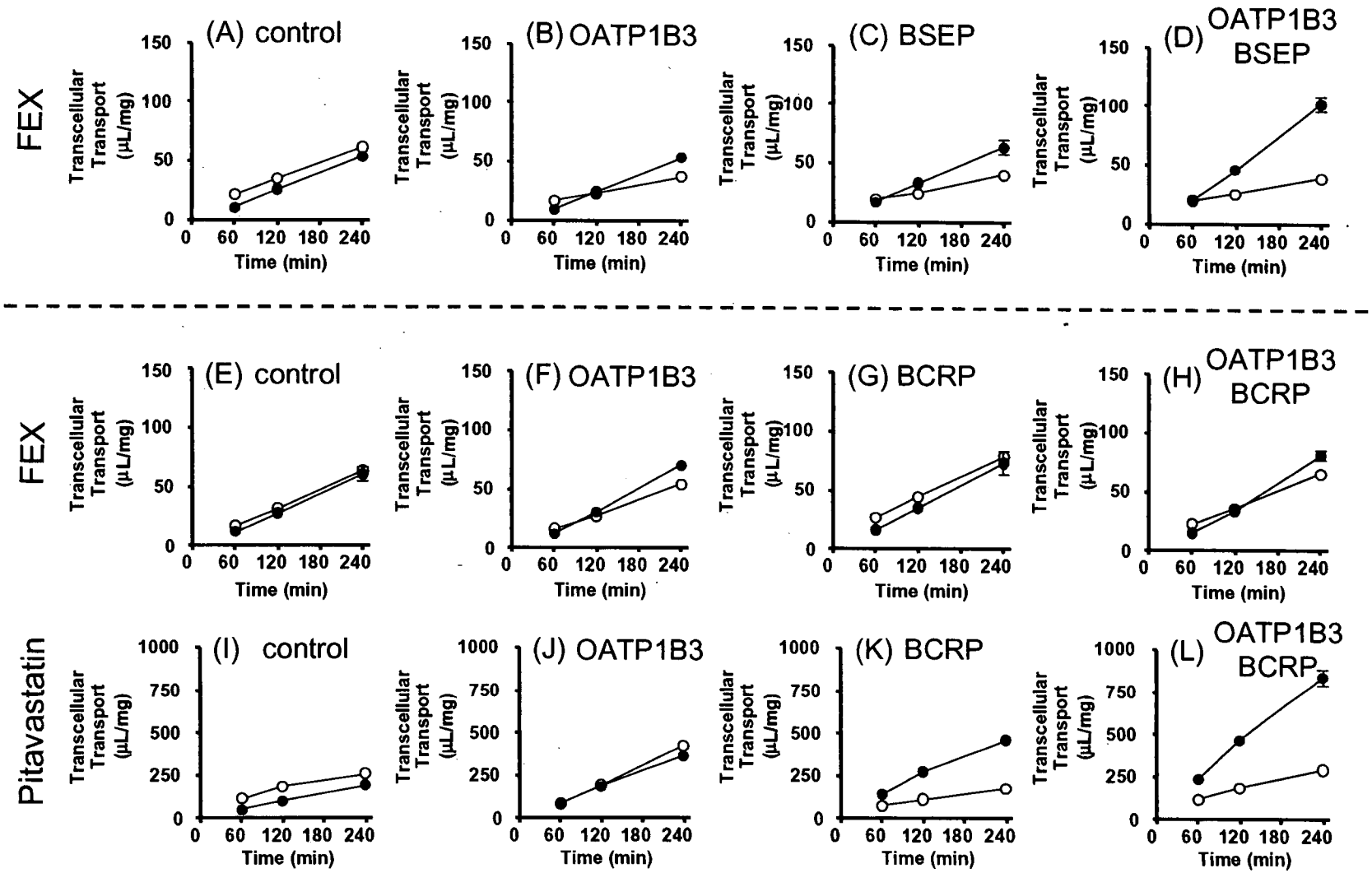
FEX
Pitavastatin
(A) control
(B) OATP1B3
(C) BSEP
(D) OATP1B3 BSEP
(E) control
(F) OATP1B3
(G) BCRP
(H) OATP1B3 BCRP
(I) control
(J) OATP1B3
(K) BCRP
(L) OATP1B3 BCRP
Transcellular Transport (μL/mg)
Time (min)
0
60
120
180
240
50
100
150
250
500
750
1000

Figure 2

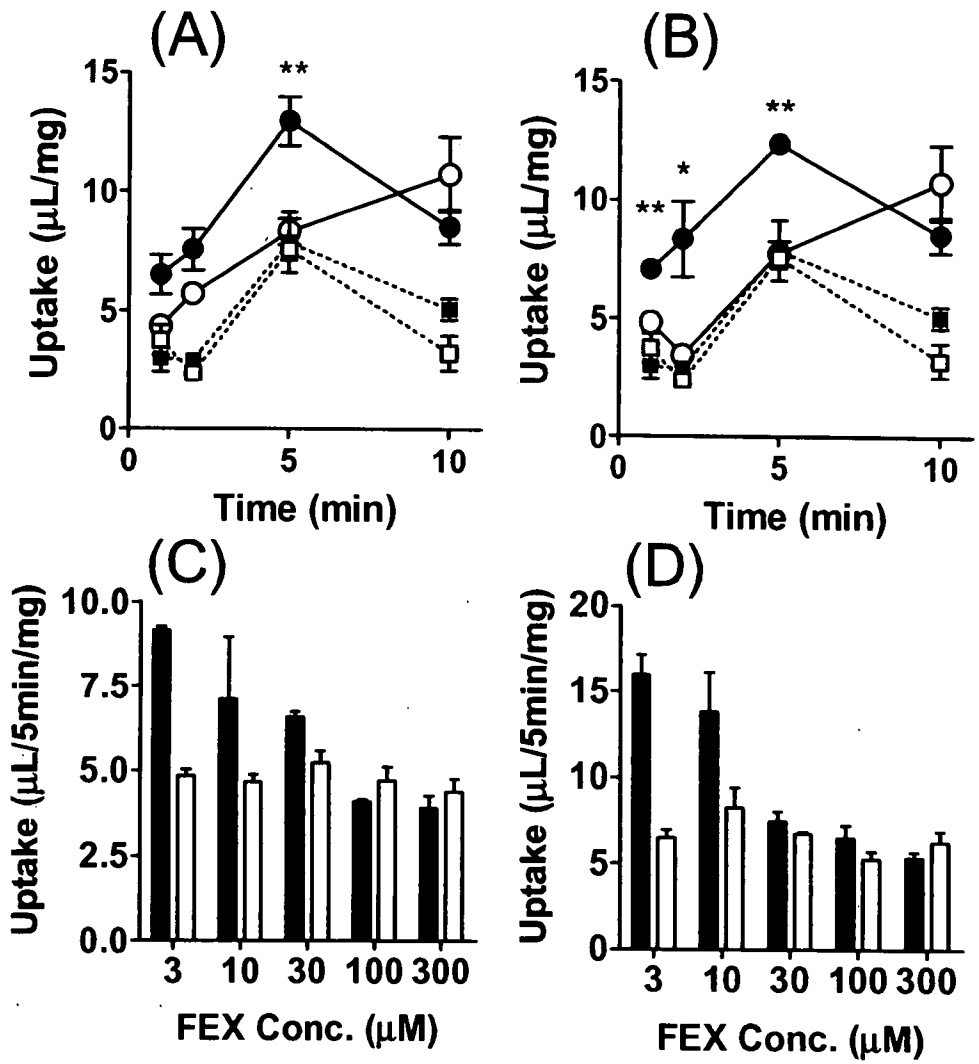
(A)
(B)
(C)
(D)
Uptake (µL/mg)
Time (min)
Uptake (µL/5min/mg)
FEX Conc. (µM)
3 10 30 100 300
0 5 10
0 5 10 15
0.0 2.5 5.0 7.5 10.0
0 5 10 15 20
* **

Figure 3

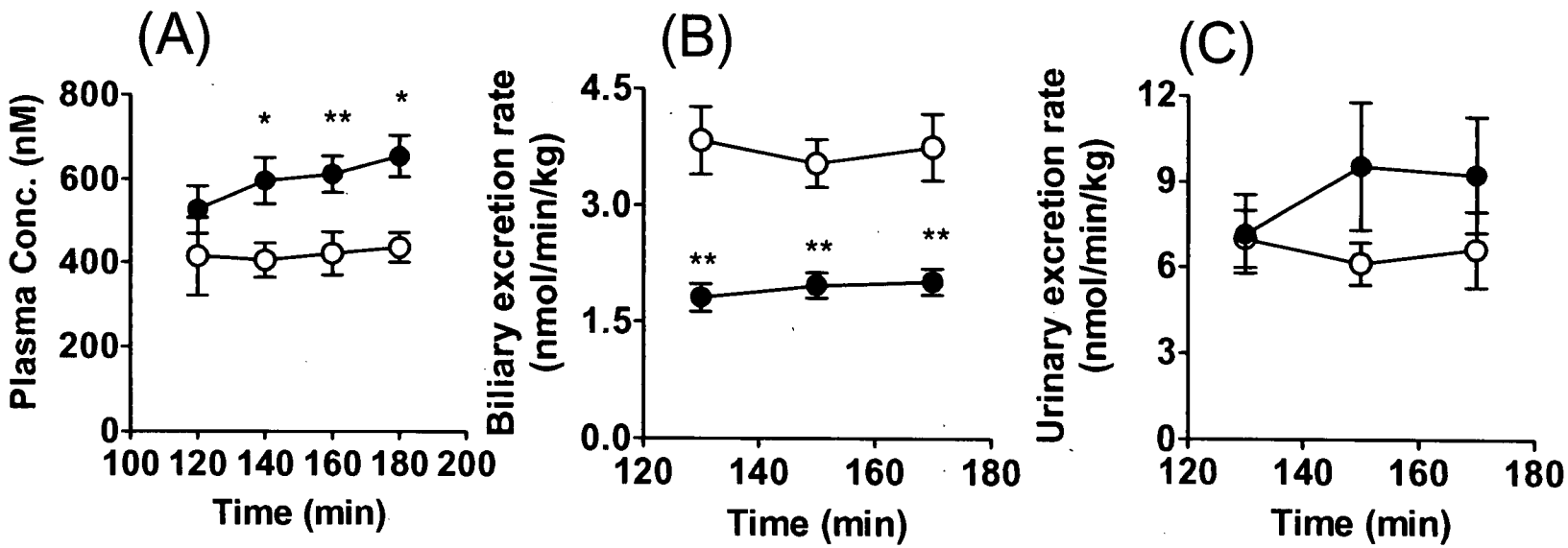
(A)
Plasma Conc. (nM)
800
600
400
200
0
100 120 140 160 180 200
Time (min)
*
**
*
(B)
Biliary excretion rate (nmol/min/kg)
4.5
3.0
1.5
0.0
120 140 160 180
Time (min)
**
**
**
(C)
Urinary excretion rate (nmol/min/kg)
12
9
6
3
0
120 140 160 180
Time (min)

Figure 4

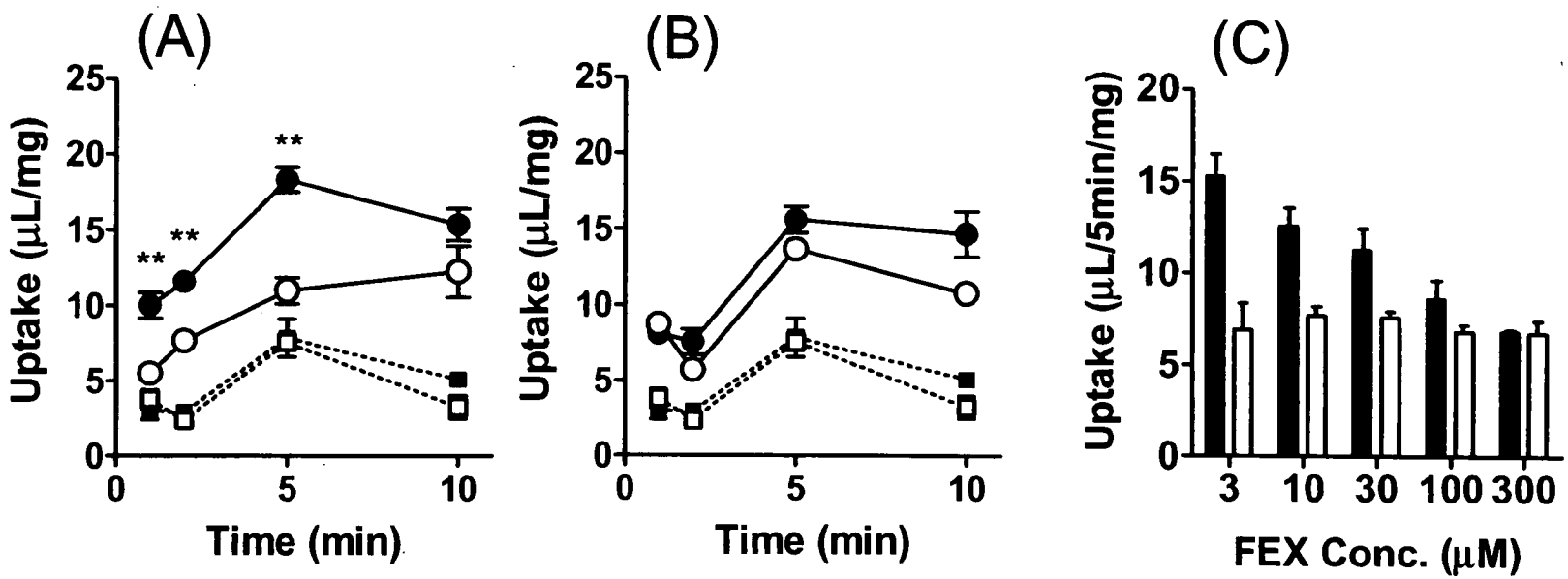
(A)
Uptake (µL/mg)
25
20
15
10
5
0
0
5
10
Time (min)
**
**
**
(B)
Uptake (µL/mg)
25
20
15
10
5
0
0
5
10
Time (min)
(C)
Uptake (µL/5min/mg)
20
15
10
5
0
3
10
30
100
300
FEX Conc. (µM)

Figure 5

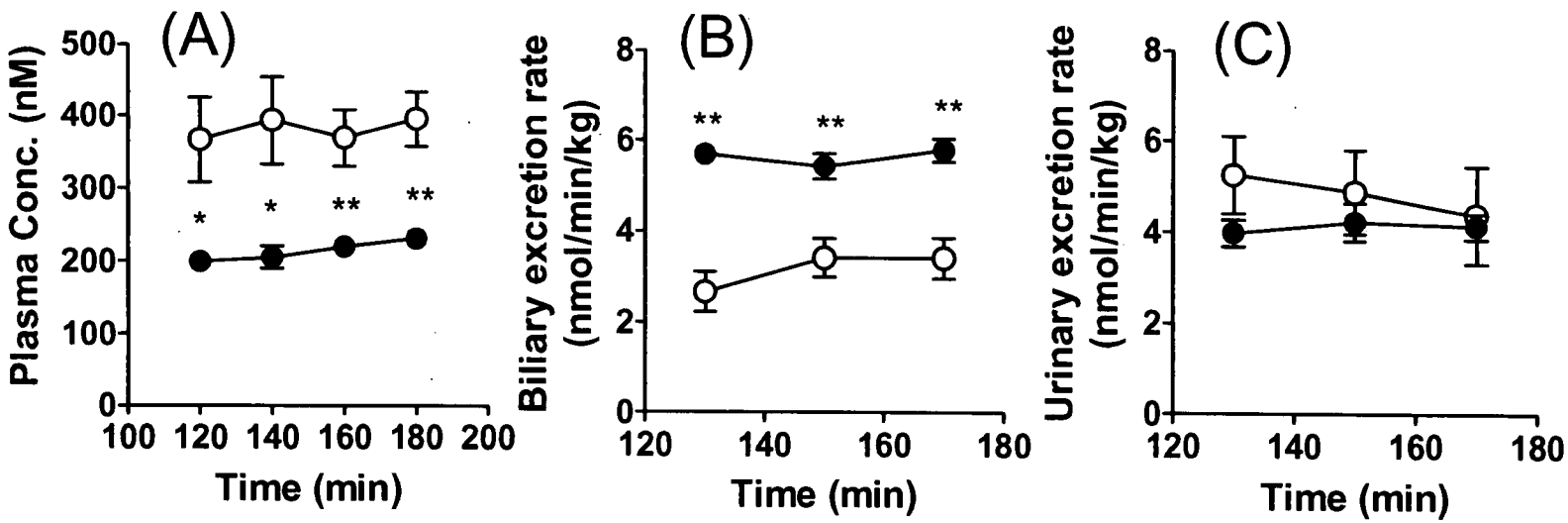
(A)
Plasma Conc. (nM)
500
400
300
200
100
0
100 120 140 160 180 200
Time (min)
*
*
**
**
(B)
Biliary excretion rate (nmol/min/kg)
8
6
4
2
0
120 140 160 180
Time (min)
**
**
**
(C)
Urinary excretion rate (nmol/min/kg)
8
6
4
2
0
120 140 160 180
Time (min)

Figure 6

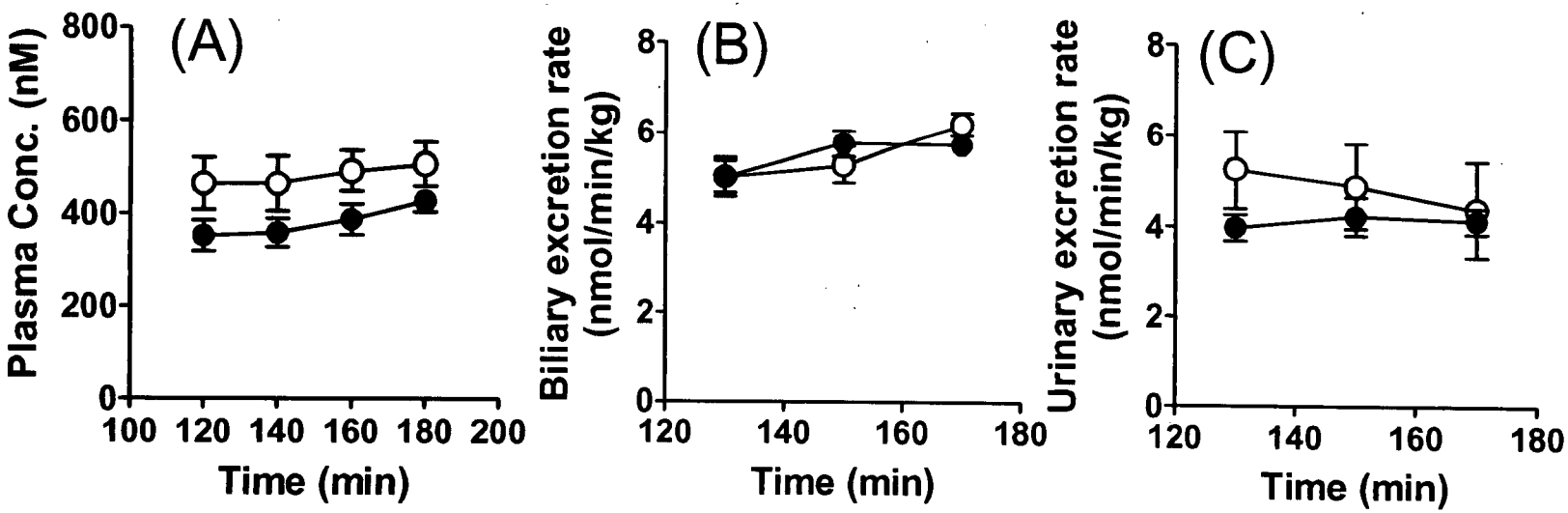
(A)
Plasma Conc. (nM)
800
600
400
200
0
100 120 140 160 180 200
Time (min)
(B)
Biliary excretion rate (nmol/min/kg)
8
6
4
2
0
120 140 160 180
Time (min)
(C)
Urinary excretion rate (nmol/min/kg)
8
6
4
2
0
120 140 160 180
Time (min)

Figure 7

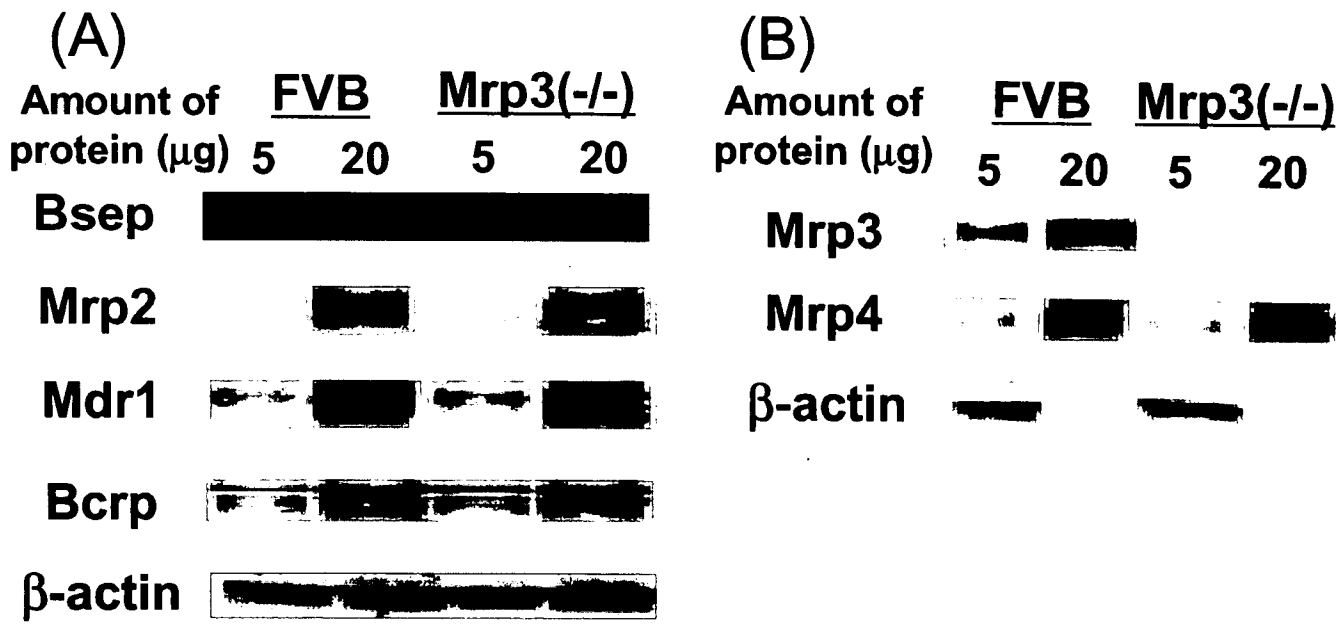
(A)
Amount of protein (μg)
FVB
Mrp3(-/-)
5
20
5
20
Bsep
Mrp2
Mdr1
Bcrp
β-actin
(B)
Amount of protein (μg)
FVB
Mrp3(-/-)
5
20
5
20
Mrp3
Mrp4
β-actin

Figure 8

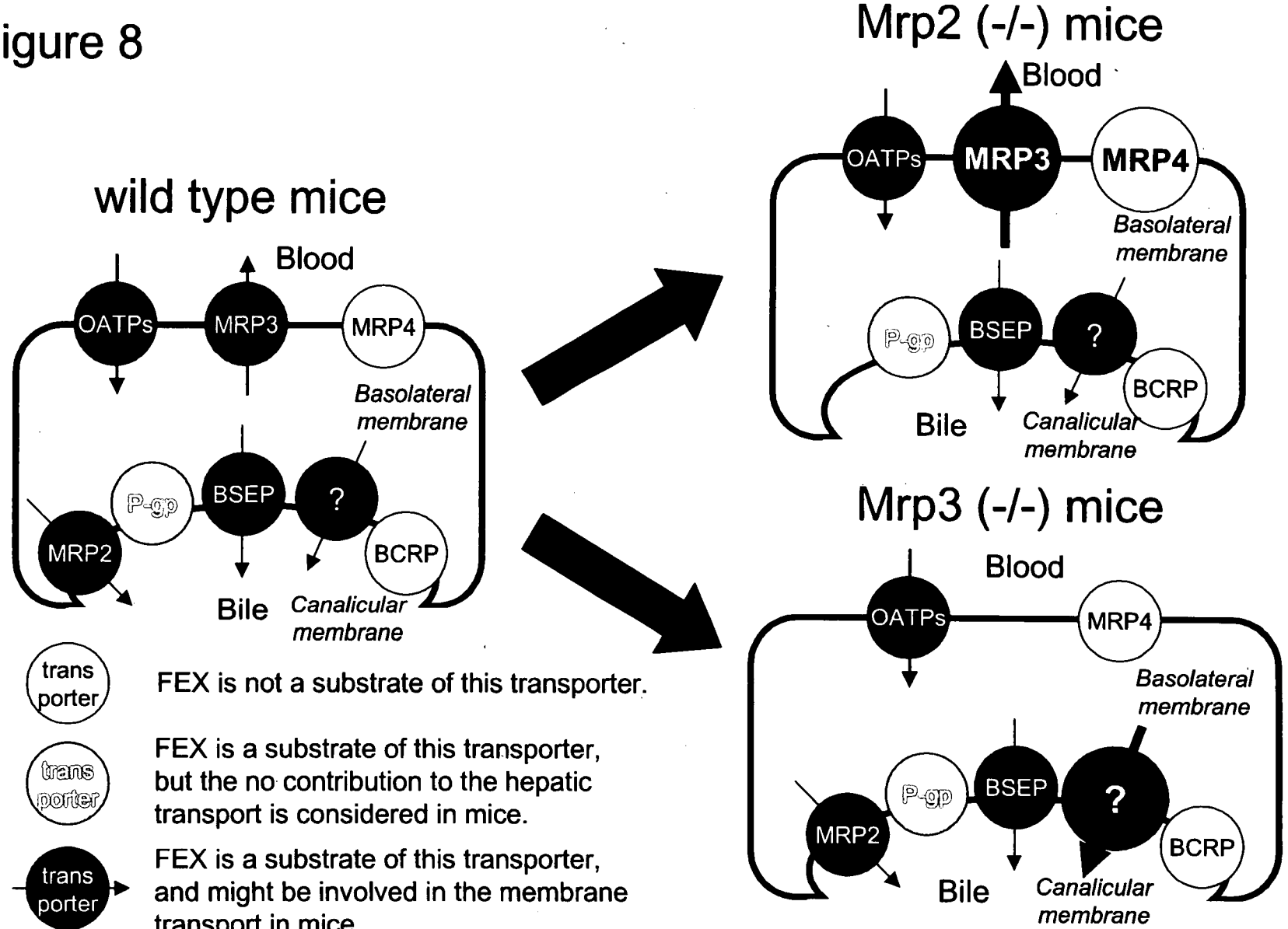
wild type mice
Blood
OATPs
MRP3
MRP4
Basolateral membrane
P-gp
BSEP
?
MRP2
BCRP
Bile
Canalicular membrane
Mrp2 (-/-) mice
Blood
OATPs
MRP3
MRP4
Basolateral membrane
P-gp
BSEP
?
BCRP
Bile
Canalicular membrane
Mrp3 (-/-) mice
Blood
OATPs
MRP4
Basolateral membrane
P-gp
BSEP
?
MRP2
BCRP
Bile
Canalicular membrane
trans porter
FEX is not a substrate of this transporter.
trans porter
FEX is a substrate of this transporter, but the no contribution to the hepatic transport is considered in mice.
trans porter
FEX is a substrate of this transporter, and might be involved in the membrane transport in mice.

0022-3565/08/3242-784–790
THE JOURNAL OF PHARMACOLOGY AND EXPERIMENTAL THERAPEUTICS
U.S. Government work not protected by U.S. copyright
JPET 324:784–790, 2008

Vol. 324, No. 2
128249/3301426
Printed in U.S.A.

Transcriptional Regulation of Human and Mouse Organic Anion Transporter 1 by Hepatocyte Nuclear Factor 1 α/β

Takami Saji, Ryota Kikuchi, Hiroyuki Kusuhara, Insook Kim, Frank J. Gonzalez, and Yuichi Sugiyama

Department of Molecular Pharmacokinetics, Graduate School of Pharmaceutical Sciences, University of Tokyo, Tokyo, Japan (T.S., R.K., H.K., Y.S.); and Laboratory of Metabolism, National Cancer Institute, National Institutes of Health, Bethesda, Maryland (I.K., F.J.G.)

Received July 6, 2007; accepted November 19, 2007

ABSTRACT

Organic anion transporter 1 (OAT1/*SLC22A6*) is predominantly expressed in the proximal tubules of the kidney. Cumulative studies have shown its critical role in the tubular secretion of a variety of organic anions, including several clinically important drugs. In addition, OAT1 is also involved in the pharmacological effect of diuretics and the nephrotoxicity of antiviral drugs. In contrast to these functional characterizations, the regulatory mechanism of OAT1 expression is poorly understood. It was recently demonstrated that the expression of Oat1 was markedly reduced in the kidneys of hepatocyte nuclear factor 1α (Hnf1α)-null mice. However, in vitro evidence for the involvement of HNF1α and further analyses are required to illustrate the transcriptional regulation of *OAT1* genes in more detail. Computational analysis of the potential transcription factor binding sites revealed that the HNF1-motif was conserved in the proximal-promoter region of human and mouse *OAT1* genes. The mRNA expression of mouse organic anion transporter 1 was drastically reduced in Hnf1α-null mice compared with that in wild-type mice, which was consistent with a previous report (Maher et al., 2006). Forced expression of HNF1α alone or both HNF1α and HNF1β enhanced the activity of human and mouse OAT1 promoters in the transactivation assays, whereas HNF1β alone was not active. Mutations in the HNF1-motif significantly reduced this transactivation. Direct binding of HNF1α/HNF1α homodimer and HNF1α/HNF1β heterodimer to the HNF1-motif found in the human OAT1 promoter was demonstrated by electrophoretic mobility shift assays. These results provide convincing evidence for the involvement of HNF1α/β in the constitutive expression of human and mouse OAT1 in the kidney.

Secretary transport from blood to urine across the renal proximal tubules is an important pathway in the renal elimination of many compounds, including both endobiotics and xenobiotics. Cumulative studies have shown that organic anion transporter 1 (OAT1/*SLC22A6*) and organic anion transporter 3 (OAT3/*SLC22A8*) account for the uptake of anionic compounds from the systemic circulation into the renal proximal-tubular epithelial cells at the basolateral membrane (Enomoto and Endou, 2005; Sekine et al., 2006). So far, many groups, including us, have characterized the transport properties of OAT1 and OAT3 and demonstrated that several drugs, such as β-lactam antibiotics, nonsteroidal anti-inflammatory drugs, antiviral drugs, and loop and thiazide diuretics are substrates of these transporters. Generation of Oat1- and Oat3-null mice confirmed the essential role of these transporters in the renal secretion of drugs (Sweet et al., 2002; Eraly et al., 2006). The impairment in Oat1 function in the kidney affects not only the tubular secretion of drugs but also their pharmacodynamics. For instance, loss of Oat1 in the kidney results in the reduced secretion of furosemide, leading to attenuation of the diuretic effect of this drug. It was also suggested that the accumulation of antiviral drugs, adefovir and cidofovir, in the kidney via OAT1 is associated with their nephrotoxicity (Ho et al., 2000; Cihlar et al., 2001). In contrast to these functional characterizations, information about the mechanism underlying the kidney-specific expression of OAT1 remains limited.

We have recently characterized the transcriptional regulation of OAT3 and urate transporter 1 (URAT1/*SLC22A12*) and shown that the coordinated action of hepatocyte nuclear factor 1 α/β (HNF1α/β) and DNA methylation determines the kidney-specific expression of these transporters (Kikuchi et

T.S. and R.K. contributed equally to this work.

Article, publication date, and citation information can be found at http://jpet.aspetjournals.org.
doi:10.1124/jpet.107.128249.

ABBREVIATIONS: OAT, organic anion transporter; URAT, urate transporter; HNF, hepatocyte nuclear factor; hOAT, human OAT; PCR, polymerase chain reaction; mOat, mouse organic anion transporter; GAPDH, glyceraldehyde-3-phosphate dehydrogenase; bp, base pair; HEK, human embryonic kidney; wt, wild type; mut, mutated wild-type sequence; EMSA, electrophoretic mobility shift assay.

al., 2006, 2007). HNF1 consists of two isoforms, HNF1α and HNF1β, and activates the transcription of target genes via direct binding to their promoters after forming homodimers or heterodimers between the two isoforms (Mendel and Crabtree, 1991; Tronche and Yaniv, 1992). These transcription factors were originally identified to be involved in the maintenance of hepatic gene expression, such as albumin, α1-antitrypsin, and α- and β-fibrinogen, as well as some of the organic anion transporters in the liver (Shih et al., 2001). As a result, cumulative reports including the analyses of gene-disrupted animals suggest the importance of HNF1α/β in extrahepatic organs, such as the pancreas and kidney (Pontoglio et al., 1996; Lee et al., 1998; Gresh et al., 2004).

In the kidney, HNF1α exhibits restricted distribution within the proximal tubules, whereas HNF1β is expressed along the entire nephrons (Lazzaro et al., 1992; Pontoglio et al., 1996). HNF1 normally exists as the HNF1α/HNF1β heterodimer or HNF1β/HNF1β homodimer in the proximal tubules, whereas HNF1β/HNF1β homodimer is predominantly expressed in the other segments. As for renal organic anion transporters, mRNA expression of Oat1, as well as Oat2 and Oat3 in the kidney, is reduced in Hnf1α-null mice, suggesting the role of HNF1α in the transcription of organic anion transporters not only in the liver but also in the kidney (Maher et al., 2006). Computational analysis of the human and mouse OAT1 5′-flanking sequences revealed that the HNF1-motif is conserved in the proximal-promoter region of *OAT1* genes (Fig. 1). On the other hand, Ogasawara et al. (2007) recently reported that HNF4α, an orphan member of the nuclear receptor superfamily, enhances the promoter activity of human OAT1, whereas the effect of HNF1α or HNF1β was minimal. HNF4α forms homodimers to bind to a DNA sequence corresponding to a direct repeat of AGGTCA-like hexamers separated by one or two nucleotides (DR1 or DR2, respectively) or an inverted repeat of the hexamers separated by eight nucleotides (IR-8) (Sladek et al., 1990; Fraser et al., 1998; Prieur et al., 2005) and regulates the hepatic expression of human organic anion transporter 2 (*SLC22A7*) and organic cation transporter 1 (*SLC22A1*) under both physiological and pathological conditions (Popowski et al., 2005; Saborowski et al., 2006). Although HNF4α is found in the proximal tubules in the kidney (Jiang et al., 2003), the physiological significance of HNF4α in the kidney is poorly recognized due to the embryonic death of Hnf4α-null mice (Chen et al., 1994). Furthermore, it has yet to be investigated whether HNF1α/β is actually involved in the transcription of the human *OAT1* gene, as is the case with OAT3 and URAT1.

In accordance, the purpose of the present study was to examine whether HNF1α and/or HNF1β is involved in the transcriptional regulation of human and mouse *OAT1* genes and to further confirm the importance of HNF1 in the regulation of organic anion transporters in the kidney.

Materials and Methods

Materials. All reagents were purchased from Wako Pure Chemicals (Osaka, Japan) unless stated otherwise.

Preparation of Total RNA and Quantitative Polymerase Chain Reaction. Total RNA was isolated from the kidney of 7 to 14-week-old male (n = 3) and female (n = 4) wild-type or Hnf1α-null mice (Lee et al., 1998), and it was treated with DNase I to eliminate the contaminated genomic DNA. The total RNA was reverse-transcribed using a random-nonamer primer (Takara, Shiga, Japan), and real-time quantitative polymerase chain reaction (PCR) was performed as previously described (Kikuchi et al., 2006) using the primers shown in Table 1 to quantify the mRNA expression of mouse organic anion transporter 1 (mOat1). The mRNA expression of mOat1 was normalized by the mRNA expression of GAPDH and statistically analyzed by the Student's t test.

Isolation of the 5′-Flanking Region of the *hOAT1* and *mOat1* Genes. The transcriptional start site of the *hOAT1* and *mOat1* gene was identified based on the information in the public database, Database of Transcriptional Start Sites (http://dbtss.hgc.jp/), with the reference sequence identification for *hOAT1* and *mOat1* (NM_004790 and NM_008766, respectively). The position of the potential transcription factor binding sites in human and mouse OAT1 promoter regions was determined using MatInspector (http://www.genomatix.de/) or NUBIScan (http://pages.unibas.ch/wtt/Products/Nubiscan/nubiscan.html) (Podvinec et al., 2002). The 919- and 110-base pair (bp) 5′-flanking regions of the human and mouse *OAT1* gene were amplified by PCR using human and mouse genomic DNA as a template, respectively. An artificial KpnI or HindIII restriction site was added to the primer sequences, which are shown in Table 1. The PCR products were digested with KpnI and HindIII after subcloning into pGEM-T Easy vector (Promega, Madison, WI) and ligated into pGL3-Basic vector (Promega) predigested with KpnI and

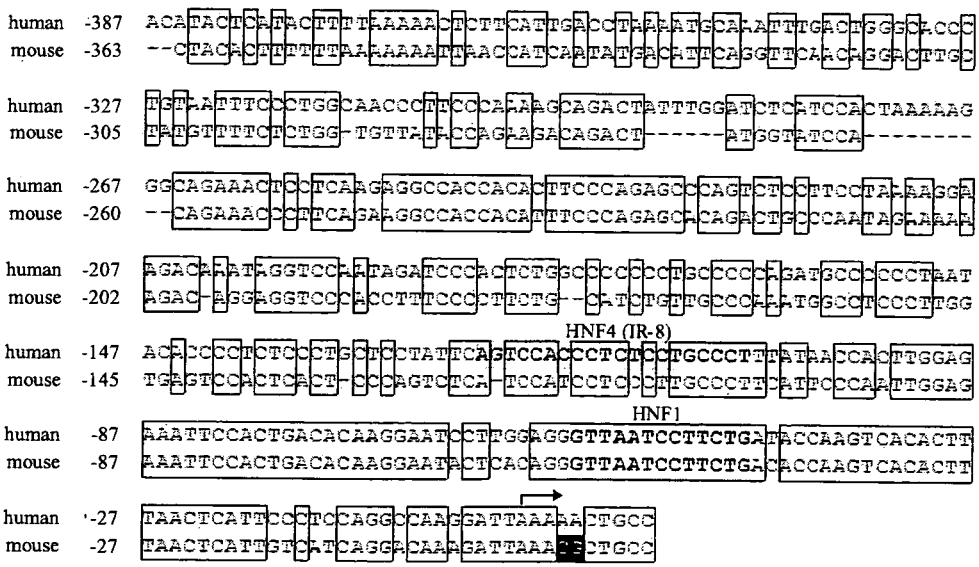

Fig. 1. Alignment of the proximal promoters of human and mouse *OAT1* genes. Nucleotide sequences of human and mouse OAT1 promoter regions were aligned using Genetyx-win version 8 software to illustrate the high homology of the 5′-flanking sequences between species. Nucleotide numberings are relative to the transcriptional start sites indicated by an arrow (+1), and homologous sequences between species are boxed. The putative HNF1-motif and the IR-8 element are shaded, and CpG dinucleotides in each sequence are reverse-colored.